Orbital contribution to the $3d$ magnetic moment in ferromagnetic Cu$_3$Au-type transition-metal-Pt alloys probed by soft-x-ray magnetic circular dichroism

S. Imada, T. Muro, T. Shishidou,* and S. Suga

Division of Material Physics, Graduate School of Engineering Science, Osaka University, 1-3, Machikaneyama, Toyonaka 560-8531, Japan

H. Maruyama, K. Kobayashi,[†] and H. Yamazaki

Faculty of Science, Okayama University, 3-1-1 Tsushimanaka, Okayama 700-8530, Japan

T. Kanomata

Faculty of Engineering, Tohoku Gakuin University, 1-13-1 Chuo, Tagajo 985-8537, Japan

(Received 14 October 1998)

Magnetic circular dichroism in the soft-x-ray absorption spectrum in the $2p \rightarrow 3d$ excitation region of the transition-metal element is measured for ferromagnetic Cu$_3$Au-type alloys, MnPt$_3$, Fe$_3$Pt and CoPt$_3$. The electronic state, especially the contribution of the spin and orbital angular momenta to the magnetic moment, is discussed by analyzing the results. The condition for the orbital angular momentum to make a large contribution to the magnetic moment in a metallic system is discussed in terms of the degree of the localization of the $3d$ orbital, the filling of it, and the symmetry around it. [S0163-1829(99)00213-1]

I. INTRODUCTION

$3d$ transition metals and Pt make binary alloys in a wide range of concentration ratios and these alloys have various magnetic properties. At stoichiometric compositions, there often exist ordered phases. When the transition metal (represented by T) is one of the elements among Mn through Ni, ordered TPt has CuAuI-type (or $L1_0$) structure and TPt$_3$ and T_3Pt have Cu$_3$Au-type (or $L2_1$) structure.[1,2] Among the Cu$_3$Au-type ordered alloys with $T=$ Mn–Ni, ferromagnetism is found for MnPt$_3$,[3] Fe$_3$Pt,[4] CoPt$_3$,[5] and Ni$_3$Pt. This series is quite interesting in at least two points. The first point is the contrast between TPt$_3$ and T_3Pt, namely that the $3d$ electron of the transition metal is expected to be relatively localized in the former and itinerant in the latter. The second point is the change of the filling of the $3d$ orbital from $T=$ Mn to Ni. From a view point of application, magneto-optical effect and magnetic anisotropy have been studied for films of MnPt$_3$ and CoPt$_3$.[6,7] On the other hand, Fe$_3$Pt is known to show the Invar effect.[8]

Magnetic circular dichroism (MCD) of core-level absorption spectrum (XAS), namely the difference of the spectra between parallel and antiparallel geometries of the sample magnetization and the photon spin of the incident circularly polarized light, has recently been used for the study of ferromagnetic materials. XAS is not only an element-specific method but it also yields information about a specific orbital, to which the core electron is strongly excited due to the selection rule and the transition probability. For the transition metal, the $3d$ orbital, which is the main origin of the magnetic moment, can be probed by $2p$ and $3p$ XAS.

The origin of the MCD in XAS can be summarized as follows.[9] First, a circularly polarized photon selectively excites an electron with an orbital angular momentum parallel (antiparallel) to the photon spin when the azimuthal quantum number l is increased (decreased) by the photoexcitation. Second, the non-s core level has, in addition, spin-orbit interaction, which aligns the electron's spin and orbital angular momenta parallel or antiparallel to each other. Now, in a ferromagnetic material, a valence orbital has a magnetic moment, which means that the occupation of the orbital is polarized in spin and/or orbital angular momenta. The photoabsorption transition can occur only when the state to which the electron is excited is empty. The unbalance of the occupation of the valence orbital in spin and orbital angular momenta is reflected in the dependence of the absorption intensity on whether the photon spin is parallel or antiparallel to the magnetization. XAS-MCD for a core level with a large spin-orbit splitting, for example, the $2p$ level of the transition-metal elements, is particularly a good tool since, in such a case, the circularly polarized photon select both orbital angular momentum and spin of the core electron.

The two sum rules known as the l_z sum rule[10] and the s_z sum rule[11] make use of these features of MCD and yield $\langle l_z \rangle$ and $\langle s_z \rangle$ of the valence orbital by integrating the XAS with each circular polarization. The s_z sum rule can only be used when spin-orbit splitting of the core level is large.

In T-Pt alloys, magnetic moments are carried mainly by T $3d$ electrons but the contribution of the Pt $5d$ electrons is not negligible. Spin and orbital angular momenta of the Pt $5d$ orbital were studied using the MCD in Pt $2p \rightarrow 5d$ XAS (Ref. 12) and Pt $4f \rightarrow 5d$ XAS.[13]

In this paper, we report MCD in T $2p \rightarrow 3d$ XAS of MnPt$_3$, Fe$_3$Pt, and CoPt$_3$. Our aim is to investigate the electronic and magnetic state of the T $3d$ orbital. By using the sum rules, contributions of the spin and orbital angular momenta to the magnetic moment are estimated. We discuss what determines the degree to which the orbital mo-

PRB <u>59</u>   8752

mentum contributes to the magnetic moment in a metallic system, and apply this argument to the present systems.

II. EXPERIMENT

The $MnPt_3$, Fe_3Pt, and $CoPt_3$ samples were prepared by the arc-melting method under an Ar atmosphere. The Cu_3Au ordered phase was realized by a suitable thermal treatment and was verified by x-ray powder diffraction.

The measurements of the MCD in the $2p$ XAS were performed at the beam-line NE-1B of the Accumulation Ring of the Photon Factory in the High Energy Accelerator Research Organization in Tsukuba, Japan. The clean surface of the sample was obtained by scraping *in situ* in an ultrahigh vacuum of about 5×10^{-10} Torr. The sample was cooled to below 120 K using a liquid-nitrogen cryostat. The circularly polarized soft x-ray from the helical undulator was monochromatized and incident normally on the sample. The degree of circular polarization was $95 \pm 2\%$ according to the calculation. XAS was obtained using the total photoelectron yield method by measuring the sample current and normalizing it by the photon current. The photon current was defined by the total photoelectron yield of the gold mesh just before the measurement chamber. A magnetic field of 1.1 T was applied to the sample during the measurement by a permanent magnet. The magnetic field on the sample was reversed by setting on the optical axis one of the two permanent dipole magnets whose magnetic field is opposite to each other. The magnetic field was either parallel or antiparallel to the photon's k vector (Faraday geometry). Magnetization was reversed at each photon energy to cancel a possible drift or fluctuation of the photon current and other factors.

III. RESULTS AND DISCUSSIONS

In Figs. 1(a)–1(c), the observed $2p$ XAS for the magnetization parallel to the photon spin (defined as the I_+ spectrum) and that for magnetization antiparallel to the photon spin (I_-), and their difference spectrum ($I_{MCD} = I_+ - I_-$) are shown for $MnPt_3$ [Fig. 1(a)], Fe_3Pt [Fig. 1(b)], and $CoPt_3$ [Fig. 1(c)]. We note that, by taking the magnetization direction as the quantization axis, the negative spin corresponds to the majority spin in this paper. Each spectrum has a two-peak structure due to the spin-orbit splitting of the $2p$ core level into $j = 3/2(2p_{3/2})$ and $j = 1/2(2p_{1/2})$ sublevels. The two main peaks mainly represent the $2p_{3/2} \rightarrow 3d$ and $2p_{1/2} \rightarrow 3d$ excitations. The origin of the relative photon energy was set at the boundary between the $2p_{3/2}$ and $2p_{1/2}$ regions ($2p_{1/2}$ onset). The boundary was determined as the energy where the energy derivative of the absorption ($dI/d\varepsilon$) rises abruptly. I_- was multiplied by a constant $1 + \alpha$ so that I_+ and I_- have the same intensity in the lowest photon energy region where $2p$ absorption should be absent. $|\alpha|$ was less than 4×10^{-3}.

A. Line shape

The overall MCD features seen for the three compounds, namely positive MCD in the $2p_{3/2}$ region and negative MCD in the $2p_{1/2}$ region, are the common features for the MCD of the T $2p$ core in ferromagnets as long as the magnetic moment of the T is in the same direction as the net magnetiza-

tion. The origin of these features is that the $3d$ orbitals with negative spin is more occupied than the positive spin. For example, in the $2p_{3/2}$ region, the $2p$ electron with positive (negative) spin is mainly excited to the $3d$ orbital in $I_+(I_-)$ due to the selection rule of the circularly polarized light and the spin-orbit interaction of the $2p$ core level. Since transition to an occupied state is forbidden, I_- is smaller than I_+ in the $2p_{3/2}$ region.

Although multiplet structures are much less conspicuous than in ionic compounds, we can still see some remaining structures due to the intra-atomic electron-electron interaction in the final state of the x-ray absorption. In $MnPt_3$, for example, structures in both XAS and MCD around -7.5 and -4.5 eV in the relative photon energy resemble the structures found in the calculation for $Mn^{2+}(3d^5)$ assuming a moderate crystal-field splitting ($10Dq \lesssim 1$ eV).[14] It might seem strange that multiplet structure is quite prominent only in $MnPt_3$. For Fe_3Pt and $CoPt_3$, however, MCD spectra approach zero much more rapidly than the XAS spectra in the higher photon energy region of $2p_{3/2}$. This is not the case in the $2p_{1/2}$ absorption region where both MCD and XAS equally have long tails on the higher photon energy side. These features are similar to those seen in the atomic calculation of MCD for high-spin d^6 and d^7 initial state without considering the $3d$ spin-orbit interaction ($z = 0$ and $\Delta = 1$ in Ref. 14), where MCD changes sign from positive to negative in the higher photon energy region of $2p_{3/2}$ while MCD is monotonously negative for $2p_{1/2}$. From these investigations, we can infer that the long tails seen in the $2p$ absorption of the metallic transition-metal compounds originate at least partially from the multiplet splitting of the $2p^5 3d^{n+1}$ states due to the electron-electron interaction.

B. Sum-rule analysis

In order to estimate quantitatively the contribution of the spin and orbital angular momenta to the magnetic moment of the transition metal, we analyze the spectra by using the sum rules.[10,11]

In the present case of $2p \rightarrow 3d$ XAS, the l_z sum rule can be written as

$$\langle l_z \rangle = -2 \frac{\int d\varepsilon (I_+ - I_-)}{\int d\varepsilon (I_+ + I_- + I_0)}, \quad (1)$$

where $\langle l_z \rangle$ is the average of the magnetic quantum number of the orbital angular momentum per $3d$ hole. I_0 is the XAS with the linearly polarized light whose polarization vector is parallel to the magnetization. The integration is taken over the whole $2p$ absorption region. The s_z sum rule is written as

$$\langle s_z \rangle + \frac{7}{2} \langle t_z \rangle$$

$$= -\frac{3}{2} \frac{\int_{j=3/2} d\varepsilon (I_+ - I_-) - 2 \int_{j=1/2} d\varepsilon (I_+ - I_-)}{\int d\varepsilon (I_+ + I_- + I_0)}, \quad (2)$$

where t_z is the z component of the magnetic dipole operator $\mathbf{t} = \mathbf{s} - 3\mathbf{r}(\mathbf{r} \cdot \mathbf{s})/|\mathbf{r}|^2$. The integration $\int_{j=3/2}(\int_{j=1/2})$ is taken only over the $2p_{3/2}(2p_{1/2})$ absorption region. By dividing Eq. (1) with Eq. (2), we obtain
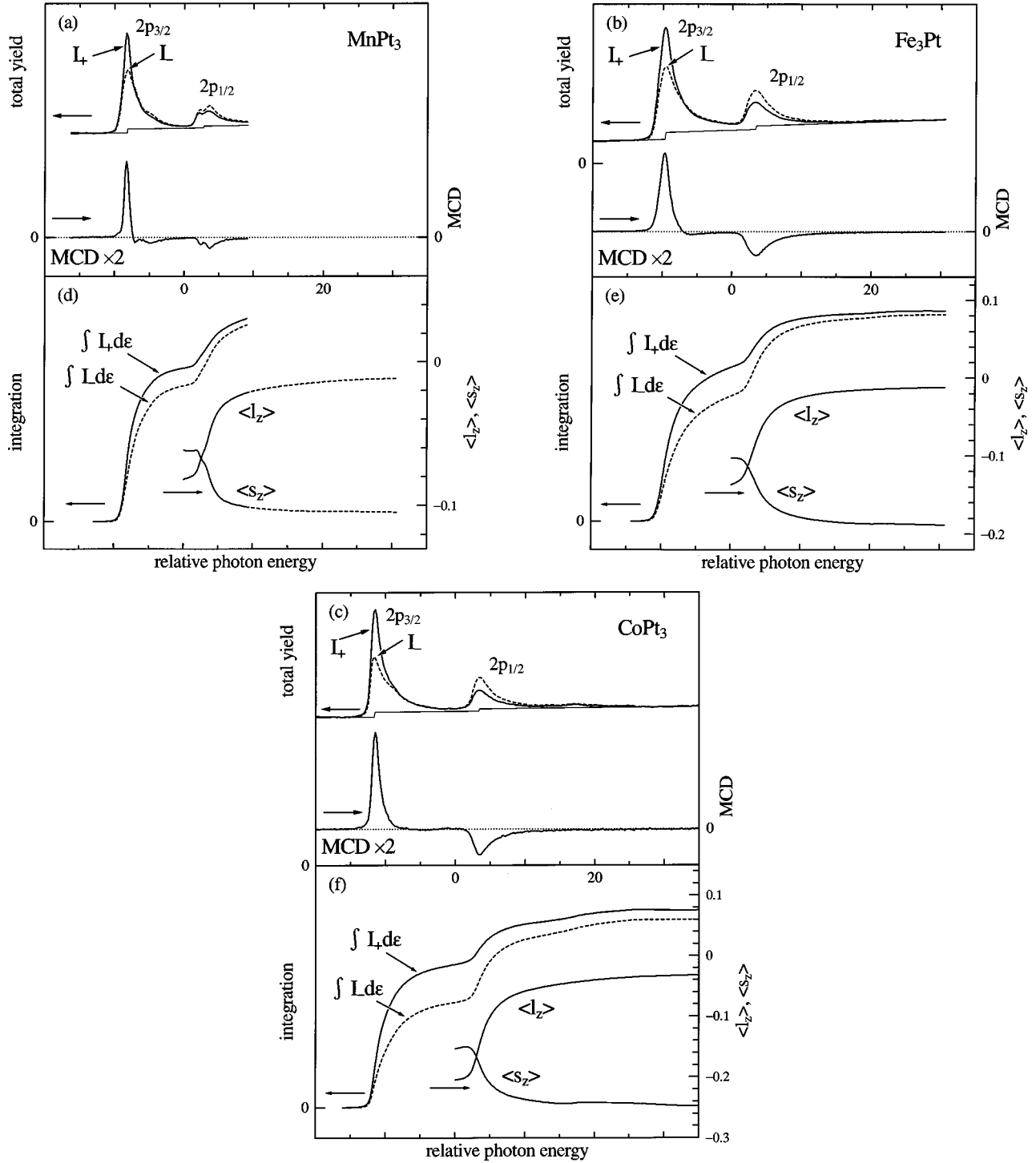
FIG. 1. (a)–(c) Upper panels: $2p$ core-level absorption spectra of Cu_3Au-type transition-metal-Pt ordered alloys for circularly polarized light with photon spin parallel (I_+) and antiparallel (I_-) to the magnetization. The background used in the integration is given by the thin solid line. Lower panels: MCD spectra defined by $I_{MCD} = I_+ - I_-$. (d)–(f) $\int I_+ d\varepsilon$ and $\int I_- d\varepsilon$: Integration of I_+ and I_- after subtracting the background. $\langle l_z \rangle$ and $\langle s_z \rangle$: Dependence of the orbital and spin angular momenta per $3d$ hole estimated by the sum rules on the upper energy limit of the integration of the $2p_{1/2}$ region. In the case of $MnPt_3$, $\langle l_z \rangle$ and $\langle s_z \rangle$ are extrapolated by dashed smooth curves.

$$\frac{\langle l_z \rangle}{\langle s_z \rangle + 7/2 \langle t_z \rangle} = \frac{4}{3} \frac{\int d\varepsilon (I_+ - I_-)}{\int_{j=3/2} d\varepsilon (I_+ - I_-) - 2 \int_{j=1/2} d\varepsilon (I_+ - I_-)}. \quad (3)$$

We should note that this equation is quite efficient. This equation stands even if the circular polarization of the light is not perfect in I_+ and I_- so long as the degree of polarization

is the same for both I_+ and I_-. This equation also stands even if the magnetization of the sample is not saturated. Another advantage of this equation is that it is defined only by the difference spectrum of MCD. It is not affected by how the background of XAS is assumed, while Eqs. (1) and (2) do depend on the background.

In order to use Eqs. (1) and (2), we should subtract back-

grounds from I_+ and I_- to obtain intensities of pure $2p \rightarrow 3d$ photoabsorption. We assume an empirical background that has a step at $2p_{3/2}$ and $2p_{1/2}$ absorption peaks and otherwise is a linear line as shown in Fig. 1. The increase of the absorption is due to the transition except for the $2p \rightarrow 3d$ transition, e.g., the $2p \rightarrow$ continuum state is taken into account by the step at the absorption peak. The height ratio between the step for the $2p_{3/2}$ peak and that for $2p_{1/2}$ is assumed to be 2 : 1, which is just the ratio of the degeneracy of the core hole state. For Fe_3Pt and $CoPt_3$, the slope of the background was determined so that the background agrees the absorption in the highest photon energy region. For $MnPt_3$, whose high-energy part could not be measured due to the lack of beam time, a comparable background was assumed.

The boundary between the $2p_{3/2}$ and $2p_{1/2}$ regions was determined and set to the origin of the photon energy as described in the beginning of Sec. III. We also have to determine the point where $2p_{3/2}$ absorption starts. This point was defined as the point where the absorption coincides with the background, namely, -12.9, -14.3, and -16.1 eV, for $MnPt_3$, Fe_3Pt, and $CoPt_3$, respectively.

In Figs. 1(d)–1(f) are shown the integrated values of the absorption after subtraction of the background, $\int I_+ d\varepsilon$ and $\int I_- d\varepsilon$, as functions of the upper energy limit to which the energy integrations are performed. $\langle s_z \rangle$ and $\langle l_z \rangle$ calculated by using these values, or in other words, obtained $\langle s_z \rangle$ and $\langle l_z \rangle$ values as functions of the upper energy limit of the integration of the $2p_{1/2}$ region, are also shown. Here, we omit $\langle t_z \rangle$ for simplicity. Although it has been shown that $\langle t_z \rangle$ is not negligible in solids,[15] analysis including $\langle t_z \rangle$ needs band-structure calculation and simulation of the MCD spectrum, which is out of our scope. We will come back to this point in Sec. III D. In the case of $MnPt_3$, the integration region dependences of $\langle s_z \rangle$ and $\langle l_z \rangle$ are extrapolated to higher energies by the use of the smooth dashed curves in Fig. 1(d). In Fig. 2(a), we present the values of $\langle l_z \rangle/(\langle l_z \rangle + 2\langle s_z \rangle)$, namely the portion of the contribution of the orbital angular momentum in the total magnetic moment of the transition-metal 3d electrons, as functions of the upper energy limit of the integration of the $2p_{1/2}$ absorption region. We note that this quantity has a profound physical meaning. Being a function of $\langle l_z \rangle/\langle s_z \rangle$ it is calculated using Eq. (3) and depends only on the MCD spectrum, $I_+ - I_-$, and does not depend on how we assume the background of the XAS. We also note that this quantity is not affected by the degree of the polarization of the light and the degree of saturation of the magnetization, both of which suppress $\langle l_z \rangle$ and $\langle s_z \rangle$. Hence, we concentrate our discussion on the compound dependence of $\langle l_z \rangle/(\langle l_z \rangle + 2\langle s_z \rangle)$.

Teramura et al.[16] argued the effect of the overlap between $2p_{3/2}$ and $2p_{1/2}$ final states on the s_z sum rule. According to their results, the s_z sum rule underestimates $\langle s_z \rangle$ by a factor which depends mainly upon the 3d electron number. The factor of the underestimation is reported to be 0.68, 0.88, 0.92, and 0.92 for 3d electron numbers of 5, 6, 7, and 8, respectively. According to the band-structure calculations by Shirai,[17] occupation of the 3d electronic state, i.e., the 3d electron number divided by the number of the 3d states within the muffin-tin sphere, is 55% for $MnPt_3$ and 76% for
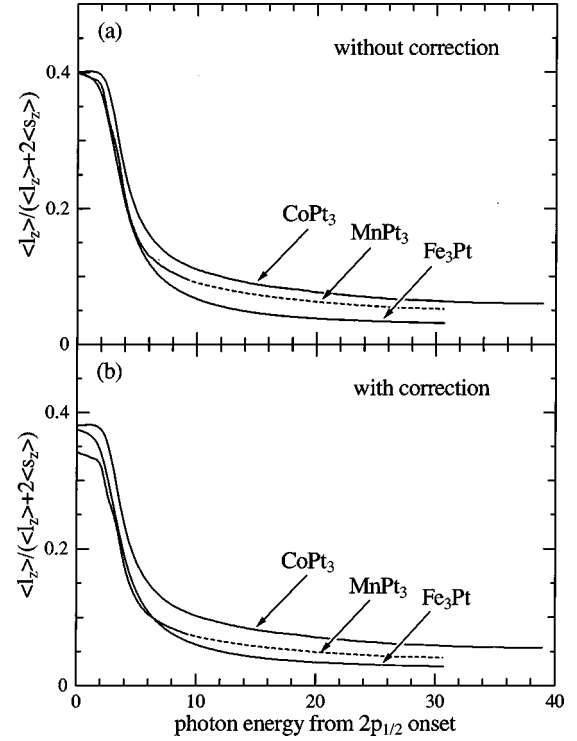
FIG. 2. (a) The contribution of the orbital angular momentum to the magnetic moment of the 3d electrons estimated by the sum rule as a function of the upper energy limit of the integration of the $2p_{1/2}$ region. (b) As for (a) but after the correction of the underestimation of $\langle s_z \rangle$ due to the overlap between $2p_{3/2}$ and $2p_{1/2}$ regions. $\langle s_z \rangle$ is assumed to be underestimated by a factor of 0.78, 0.90, and 0.92 in the case of $MnPt_3$, Fe_3Pt, and $CoPt_3$.

$CoPt_3$. We therefore assume that the 3d electron number is 5.5 and 7.6 for $MnPt_3$ and $CoPt_3$, respectively. We furthermore assume that it is 6.5 for Fe_3Pt. By linearly interpolating the values obtained by Teramura et al. we consider the factor of underestimation of $\langle s_z \rangle$ is 0.78, 0.90, and 0.92 for $MnPt_3$, Fe_3Pt, and $CoPt_3$, respectively. Figure 2(b) shows the dependence of the values of $\langle l_z \rangle/(\langle l_z \rangle + 2\langle s_z \rangle)$ on the integration region after correcting the $\langle s_z \rangle$ value by dividing it with the factors above.

The integration region dependence of $\langle s_z \rangle$ and $\langle l_z \rangle$ in Figs. 1(d)–1(f) indicates that convergence, especially of $\langle l_z \rangle$, is quite slow. The value of $\langle l_z \rangle/(\langle l_z \rangle + 2\langle s_z \rangle)$, therefore, crucially depends upon the integration region. If we take this into account, it is desirable to take as wide an integration region as possible. However, doing so would integrate the possible errors in the normalization and the background. Although $\langle l_z \rangle/(\langle l_z \rangle + 2\langle s_z \rangle)$ is free from error in the background, it is not free from that in the before-mentioned normalization between I_+ and I_-. In order to estimate the $\langle l_z \rangle/(\langle l_z \rangle + 2\langle s_z \rangle)$ value, the integration should hence be cut at some appropriate point. If we set this point to 25 eV above the $2p_{1/2}$ onset and by using the corrected values in Fig. 2(b), $\langle l_z \rangle/(\langle l_z \rangle + 2\langle s_z \rangle)$ is 0.044, 0.031, and 0.063 for the transition-metal 3d holes in $MnPt_3$, Fe_3Pt, and $CoPt_3$, respectively. The values of $\langle l_z \rangle/(\langle l_z \rangle + 2\langle s_z \rangle)$ obtained in this way are not accurate in an absolute sense. However, it is quite meaningful to compare them between different systems.

C. What determines the strength of the orbital angular momentum

Now, we discuss what determines the degree to which the orbital angular momentum is induced in metallic systems. We treat this issue from the following three points. One is the competition between itinerancy and localization of the $3d$ electron. Another is the occupancy of the $3d$ partial density of states, and the other is the symmetry of the system around the T site.

First, we consider the case where the system can be assumed to be spherically symmetric around the T atom. In this case, all the $3d$ orbitals, for example the e_g and t_{2g}, are equivalent to each other. The $3d$ partial density of states (DOS) of such a ferromagnet may be represented by a model DOS in the upper panel of Fig. 3(a) in the absence of the spin-orbit interaction. Since we are taking the direction of the *magnetic field* as the quantization axis in this paper, ↓ corresponds to the majority spin and ↑ to the minority spin. When the spin-orbit interaction is switched on, each majority- and minority-spin partial DOS would split into subbands with a different magnetic quantum number of the orbital angular momentum, l_z. Here, we have assumed that the spin is still a good quantum number in the presence of the spin-orbit interaction. In other words, we only consider the $l_z s_z$ term. This approximation can be justified when the exchange interaction is large enough so that the $l_+ s_-$ and $l_- s_+$ terms that mix the different spin state are negligible. The energy shift of the l_z subband would be $\zeta l_z s_z$ where ζ is the spin-orbit interaction constant of the $3d$ orbital which takes a positive value. The resultant shift of the subbands is illustrated in the lower panel of Fig. 3(a), where the subbands with positive (negative) l_z are represented by the thickest (thinnest) lines.

The consequence of the present shift would be as follows. When the $3d$ partial DOS is less than half-filled, l_z subbands with positive l_z and negative (majority) spin are more occupied than the negative l_z bands. Hence, orbital angular momentum with antiparallel direction as the spin is induced in this case. When the $3d$ partial DOS is nearly half-filled, the positive $\langle l_z \rangle$ induced in the majority-spin band is cancelled by the negative $\langle l_z \rangle$ induced in the minority-spin band, which leads to very small orbital angular momentum. When the $3d$ partial DOS is more than half-filled, negative $\langle l_z \rangle$ is induced and hence the orbital angular momentum is parallel to the spin.

Now, what happens when the degree of itinerancy, and hence the bandwidth, is changed in the present case? The energy splitting due to the spin-orbit coupling is not likely to depend much upon the bandwidth. Therefore, the induced orbital angular momentum would be larger for the narrower band which has larger DOS. In other words, orbital angular momentum is more induced in a system where $3d$ electrons are more localized.

Next, we should consider the case where the symmetry around the T atom is lower than the spherical symmetry. The $3d$ orbitals are no longer equivalent to each other. Here, we consider as an example that the system is octahedral or tetrahedral around the T atom. The partial density of states of t_{2g} and that of e_g are then different from each other.
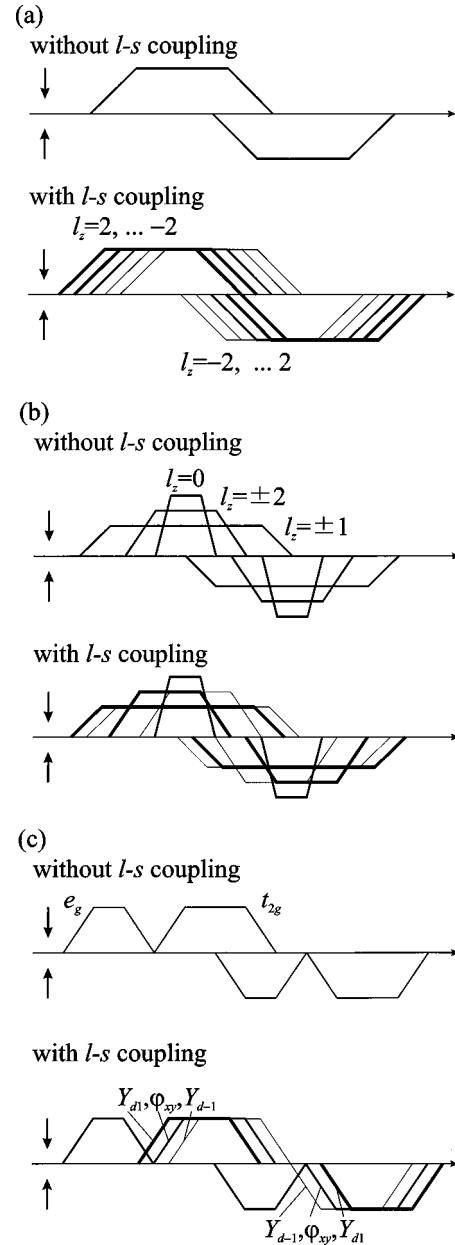
FIG. 3. Model $3d$ partial density of states (DOS) for (a) a spherically symmetric case, (b) a case where the symmetry around the transition-metal atom causes the bandwidth of the partial DOS to depend upon $|l_z|$, and (c) a case where the symmetry causes a splitting of the partial DOS into subbands. In each case, the upper panel shows the partial DOS without the spin-orbit interaction. The lower panel shows those with the spin-orbit interaction, where the thickest (thinnest) line corresponds to positive (negative) l_z.

In order to discuss the effect of the spin-orbit interaction on such a system, we should recall how the t_{2g} and e_g $3d$ states are expressed in terms of the eigenfunction of the magnetic quantum number l_z, namely the spherical harmonics Y_{dl_z}. The three t_{2g} states are expressed as $\varphi_{yz} \propto (i/\sqrt{2})(Y_{d1} + Y_{d-1})$, $\varphi_{zx} \propto -(1/\sqrt{2})(Y_{d1} - Y_{d-1})$, and $\varphi_{xy} \propto -(i/\sqrt{2})(Y_{d2} - Y_{d-2})$. The two e_g states are expressed as $\varphi_{3z^2 - r^2} \propto Y_{d0}$ and $\varphi_{x^2 - y^2} \propto (1/\sqrt{2})(Y_{d2} + Y_{d-2})$.

Let us consider the mixing between the $3d$ and the surrounding orbitals. Either of the t_{2g} or e_g states is mixed more strongly with the surroundings and hence become more itin-

erant, depending upon the crystal structure. If the t_{2g} orbital is more itinerant than the e_g orbital, for example, the $l_z = \pm 1$ states are the most itinerant since these states consist purely of t_{2g} states. $l_z = \pm 2$, which are linear combinations of the t_{2g} and e_g states, are the next and $l_z = 0$ is the most localized. This is schematically shown in the upper panel of Fig. 3(b). When the spin-orbit interaction is switched on, these bands split by energies proportional to $|l_z|$ as shown in the lower panel of Fig. 3(b). In this case, the contribution to the orbital angular momentum comes mostly from $l_z = \pm 2$, since the spin-orbit splitting of these states is stronger and the band width is narrower than $l_z = \pm 1$.

When the ionicity of the system is stronger, the center of gravity of the t_{2g} and e_g partial DOS would be quite different. The upper panel of Fig. 3(c) illustrates the partial DOS for a case where the energy of the e_g band is significantly lower than that of the t_{2g} band as when the T atom is tetrahedrally surrounded by negative ions. Linear combinations between two of the t_{2g} orbitals, φ_{yz} and φ_{zx}, lead to states with $\langle l_z \rangle \neq 0$. Namely, the $\langle l_z \rangle = \pm 1$ state is realized as $Y_{d\pm 1} \propto (1/\sqrt{2})(\frac{1}{i}\varphi_{yz} \mp \varphi_{zx})$. Therefore, when the spin-orbit interaction is switched on, the t_{2g} partial DOS split into subbands, namely, Y_{d1}, Y_{d-1}, and φ_{xy} partial DOS's as shown in the lower panel of Fig. 3(c). On the other hand, $\langle l_z \rangle$ of any linear combination of e_g states is always zero. Therefore, the e_g partial DOS would not be affected. In this situation, only the t_{2g} states contribute to the orbital angular momentum. Therefore, $\langle l_z \rangle$ is zero if the t_{2g} band is totally full or totally empty. Discussion about these aspects based on an atomic point of view was reviewed by Kanamori.[18]

D. Discussion about the present result

Now, we apply the model above to the present systems. In the Cu_3Au structure, Au is on the corner site of the fcc structure and Cu is on the face-centered site. Therefore, in both the Cu and Au sites, the t_{2g} orbital hybridizes stronger with the surrounding orbitals than the e_g orbitals. Since the structure is nearly close-packed and these systems are presumably quite metallic, the $3d$ partial DOS is considered to be like Fig. 3(b). This is qualitatively well reproduced by the band-structure calculation by Shirai.[17] Hence the orbital angular momentum should come mainly from the $l_z = \pm 2$ orbitals. This is quite consistent with the argument on TPt_3 by Iwashita et al.[19] They discussed the orbital angular momenta of the T $3d$ and Pt $5d$ orbitals on the basis that the $l_z = \pm 2$ give the largest contribution. This was deduced from their band-structure calculation based on the scalar-relativistic full-potential linear-augmented plane-wave method within the local-spin-density approximation (LSDA) with the additional inclusion of the spin-orbit interaction as a perturbation.

In $MnPt_3$ and $CoPt_3$, all the nearest neighbors of the transition-metal site are Pt sites. On the other hand, in Fe_3Pt, 2/3 of the nearest neighbors are the Fe sites and the other 1/3 are the Pt sites. Generally speaking, the Pt $5d$ partial DOS is distributed in the energy region with a significantly larger binding energy than the T $3d$ partial DOS. Therefore, the $3d$ electrons are relatively localized in $MnPt_3$ and $CoPt_3$ whereas they are quite itinerant in Fe_3Pt.

In $MnPt_3$, although the $3d$ orbital is relatively localized, it is nearly half-filled. Therefore, from our discussion in the last section it follows that the orbital angular momentum of the $3d$ electrons is expected to be small. In Fe_3Pt, although the $3d$ orbital is more than half-filled, it is quite itinerant and the orbital angular momentum is also small. In $CoPt_3$, the $3d$ orbital is more than half-filled and is relatively localized and therefore the orbital angular momentum is expected to be larger than the other two systems. This argument well explains our experimental results that the contribution of the orbital angular momentum to the magnetic moment of the $3d$ orbital is larger in $CoPt_3$ than in $MnPt_3$ and Fe_3Pt.

Finally, we quantitatively compare the contribution of the orbital angular momentum, $\langle l_z \rangle/(\langle l_z \rangle + 2\langle s_z \rangle)$, obtained in Sec. III B with that obtained by Iwashita et al.[19] According to their calculation, $\langle l_z \rangle/(\langle l_z \rangle + 2\langle s_z \rangle)$ values of the $3d$ electrons are 0.005 and 0.025 for $MnPt_3$ and $CoPt_3$, respectively. These values are significantly smaller than our values, 0.044 and 0.063, respectively. One of the origins of this discrepancy is that $\langle t_z \rangle$ is omitted in our analysis since Wu et al. showed that $\langle l_z \rangle/\langle s_z \rangle$ is overestimated by the sum-rule analysis without $\langle t_z \rangle$.[15] Another origin, of course, might be that the band-structure calculation within LSDA underestimates $\langle l_z \rangle$ since it cannot treat $\langle l_z \rangle$ self-consistently.

IV. SUMMARY

We measured the MCD in the transition-metal $2p$ absorption of the ferromagnetic Cu_3Au-type transition-metal-Pt ordered alloys, $MnPt_3$, Fe_3Pt, and $CoPt_3$. By combining the l_z and s_z sum rules, we derived $\langle l_z \rangle/(\langle l_z \rangle + 2\langle s_z \rangle)$, the portion of the orbital angular momentum's contribution to the magnetic moment of the transition-metal $3d$ orbital, for the three compounds. This quantity is not only physically important but also experimentally more reliable in the sense that it is less affected by possible extrinsic errors such as the ambiguity in the background subtraction and imperfectness in magnetization and circular polarization than individual $\langle l_z \rangle$ and $\langle s_z \rangle$. The estimated $\langle l_z \rangle/(\langle l_z \rangle + 2\langle s_z \rangle)$ values, 0.044, 0.031, and 0.063 for $MnPt_3$, Fe_3Pt, and $CoPt_3$, respectively, are still not very reliable in an absolute sense, but they are quite meaningful in a relative sense.

What determines the degree of the orbital contribution to the magnetic moment in metallic ferromagnets was discussed. The orbital contribution is enhanced when the $3d$ electrons are localized and when the $3d$ filling is far from either empty, half-filled, or fully filled. The fact that the orbital contribution is the largest in $CoPt_3$ is explained by that the $3d$ electrons are relatively localized and the $3d$ orbital is more than half-filled in it, whereas the $3d$ electron is quite itinerant in Fe_3Pt and the $3d$ orbital is nearly half-filled in $MnPt_3$.

*Present address: Department of Materials Science, Faculty of Science, Hiroshima University, Higashi-Hiroshima 739, Japan.

†Present address: Fundamental Research Laboratories, NEC Corporation, 34, Miyukigaoka, Tsukuba, Ibaraki 305-8501, Japan.

[1] J. J. M. Franse and R. Gersdorf, in *Magnetic Properties of Metals—3d, 4d and 5d Elements, Alloys and Compounds*, Landolt-Börnstein, New Series, Vol. 19a, edited by H. P. J. Wijn (Springer-Verlag, Berlin, 1986).

[2] J. G. Booth, in *Ferromagnetic Materials*, edited by E. P. Wohlfarth and K. H. J. Buschow (North-Holland, Amsterdam, 1988), Vol. 4.

[3] B. Antonini, F. Lucari, F. Menzinger, and A. Paoletti, Phys. Rev. **187**, 611 (1969).

[4] Y. Itoh, T. Sasaki, and T. Mizoguchi, Solid State Commun. **15**, 807 (1974).

[5] F. Menzinger and A. Paoletti, Phys. Rev. **143**, 365 (1966).

[6] E.T. Kulatov, Yu.A. Uspenskii, and S.V. Halilov, J. Magn. Magn. Mater. **163**, 331 (1996).

[7] M. Maret, M.C. Cadeville, R. Poisot, A. Herr, E. Beaurepaire, and C. Monier, J. Magn. Magn. Mater. **166**, 45 (1997).

[8] P. Böni, G. Shirane, B.H. Grier, and Y. Ishikawa, J. Phys. Soc. Jpn. **55**, 3596 (1986).

[9] S. Imada and T. Jo, J. Phys. Soc. Jpn. **59**, 3358 (1990).

[10] B.T. Thole, P. Carra, F. Sette, and G. van der Laan, Phys. Rev. Lett. **68**, 1943 (1992).

[11] P. Carra, B.T. Thole, M. Altarelli, and X. Wang, Phys. Rev. Lett. **70**, 694 (1993).

[12] H. Maruyama, F. Matsuoka, K. Kobayashi, and H. Yamazaki, J. Magn. Magn. Mater. **140-144**, 43 (1995).

[13] T. Shishidou, S. Imada, T. Muro, F. Oda, A. Kimura, S. Suga, T. Miyahara, T. Kanomata, and T. Kaneko, Phys. Rev. B **55**, 3749 (1997).

[14] G. van der Laan and B.T. Thole, Phys. Rev. B **43**, 13 401 (1991).

[15] R. Wu, D. Wang, and A.J. Freeman, J. Magn. Magn. Mater. **132**, 103 (1994).

[16] Y. Teramura, A. Tanaka, and T. Jo, J. Phys. Soc. Jpn. **65**, 1053 (1996).

[17] M. Shirai, Physica B **237-238**, 351 (1997); (private communication).

[18] J. Kanamori, in *Magnetism*, edited by G. T. Rado and H. Suhl (Academic, New York, 1963), p. 166.

[19] K. Iwashita, T. Oguchi, and T. Jo, Phys. Rev. B **54**, 1159 (1996); (private communication).